Development of a nonlinear model prediction control application: Implementation on a Paracetamol Batch Crystallization Process

Mariana Monteiro
mariana.i.p.monteiro@tecnico.ulisboa.pt

Instituto Superior Técnico, Lisboa, Portugal

October 2019

Abstract

This thesis presents the implementation of a Nonlinear Model Predictive Control application on a paracetamol batch crystallization process. This control strategy uses the mathematical model of the process and takes advantage of its current measurements to predict the future behaviour of some chosen Controlled Variables. The controller does this by performing an optimisation routine that minimizes the difference between the current value of the Controlled Variables and their target interval of values. In this thesis, the optimisation is described by a penalty-based objective function, in which penalties are added whenever the Controlled Variables are outside their target interval of values.

The controller was tested on a digital twin of the model, which is the real-time implementation of the controller on the process. The testing consisted in submitting the controller to different scenarios to verify whether it was able to steer the Controlled Variables into their target limits, thus, achieving their control objectives. Tested scenarios included disturbance rejection (changing Disturbance Variable impeller frequency), noise measurement (adding noise to one of the measured variables, Span) and plant / model mismatch (altering one of the kinetic parameter, supersaturation order) . The controller was able to successfully steer the Controlled Variables for most cases, yielding faster results than in open-loop mode. Reaching control objectives faster than in open-loops proves to be an advantage as it can translate in ending a batch sooner, thus saving time.

Overall, the controller yielded quite satisfactory results, showing a promising future for this less commonly used control strategy.

Keywords: Nonlinear Model Predictive Control, Batch Crystallization, Digital-twin, Optimization

1. Introduction

Model Predictive Control (MPC) is an advanced process control technique which consists in using the mathematical model of the system and its current measurements to calculate the optimal control action that satisfies the system's control objectives [1]. These control objectives are defined as certain setpoints for specific variables, called controlled variables (CVs). The controller compares the current values of the Controlled Variables and the actual ones, and optimizes what control action will minimize this difference [2]. That control action is implemented in the form of manipulated variables (MVs) setpoints. This strategy is said to be "predictive" as the controller decides the control action to implement, based on the predicted behaviour of the CVs. The concept behind this strategy is described by the following figure 1.

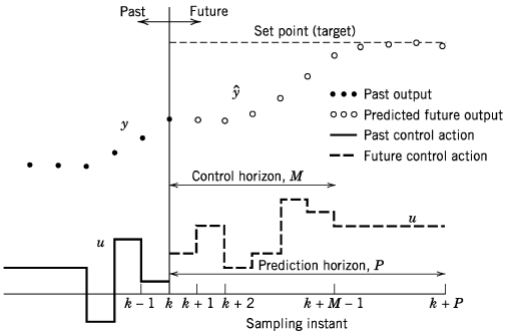

Figure 1: Model Predictive Control Concept [1]

In the shown figure, y represents the past measurements of the CVs, and ŷ the predicted measurements by the controller. The target set point refers to the CVs' desired value. The past control action, line u, represents the past control action that has been implemented by the controller, and the dashed line u the future control action to be implemented. Different MVs setpoints

will be given, over a control or optimisation horizon, M. The MVs will remain constant until the end of the prediction horizon, P, since the CVs have reached their desired value.

Ideally, the controller would be able to predict the exact behaviour of the CVs, after having implemented a certain control action. However, in reality, due to plant / model mismatch, the predicted measurements are not equal to the actual ones [3, 1]. This mismatch may be due to sensor/actuator delays or misreadings. To tackle this problem, the controller operates in cycles. After a certain period of time, the controller takes new measurements and compares the measurements of the CVs to the values it had predicted. As they do not match, the controller performs a new optimisation to take into account this new value, and corrects what it had implemented. Hence, in practice, only the first element of the optimal control sequence is applied to the system, before the calculation sequence restarts: this strategy is called the receding horizon control, and it is very advantageous as it takes into account the most recent measurements of the state [1, 4]. For variables whose measurement is not possible frequently, state estimation calculations are used.

Both the control and the prediction horizons must be carefully chosen as they influence the controller's response. The longer they are, the more time the controller has to steer its CVs into the desired setpoints. On the other hand, the shorter the horizons, the less time the controller has to satisfy its control objectives - the more abrupt the control action must be. The duration of the cycle is also an important matter as each cycle should be long enough to include relevant system's dynamics, but not so long as to miss some [2].

There are some processes for which nonlinear model predictive control seems attractive. Some characteristics of such processes include having batch reactors, frequent product requirements changes, infrequent measurements of product quality and raw-material composition fluctuations [5, 6].

The main industrial applications of NMPC are in the polymerization sector [7, 8, 9, 10, 11, 12]. Polymers have highly nonlinear dynamics, specially in the interactive reactions between the chains. Moreover, the lack of quality measurements, due to sampling problems, large dead times and high noise level also motivates the use of a model that makes use of state estimation features. Finally, given the existence of unmeasurable properties such as the chain length distribution and the average molecular mass, there is no possible way to have output measurements at every sampling intervals.

Not as developed as the polymers processes, but still with a growing implementation at research level, is the crystallization sector [13, 14, 15, 16, 17]. Similarly to polymers, crystals have quite complex mechanisms such as agglomeration, growth and nucleation, with kinetics that are not easily modelled. Likewise, crystals have immeasurable properties in real time, namely the crystal mass and the fine size distribution. In addition to that, factors like sensor limitations (in taking reliable measurements) and inherent process uncertainties [18, 19] all provide suitable reasons to implement a nonlinear advanced control strategy.

2. Crystallization

Crystallization is a very common practice in the pharmaceutical industry as a separation and purification process [13]. Its driving force lays on the difference between the chemical potential of the supersaturated solution and the solid crystal phase [18, 13, 20].

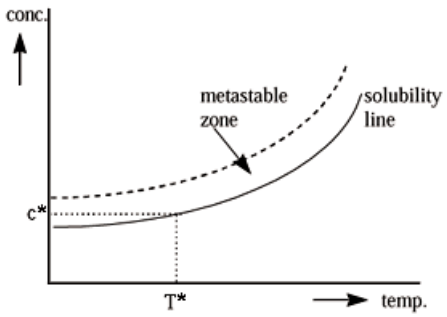

Figure 2: Solubility diagram [21]

Figure 2 shows the solubility curve for a typical API (Active Pharmaceutical Ingredient) [22]. Below the curve, it is said that the system is under saturated, as its concentration is lower than its solubility. In this case, crystals will dissolve [23]. Above the curve, the system is said to be supersaturated, given its concentration is higher than the equilibrium one. In between these two regions (solubility and dashed curves) lays the "metastable zone", where already formed crystals can grow, but it is quite unlikely to form new ones [23, 24]. In this area, the system is already supersaturated, but it is not yet able to respond to spontaneous nucleation [25] - it is the ideal area to grow, as it minimizes impurities. Supersaturation can be induced by cooling, anti-solvent addition, evaporation and pH change. [13, 18, 26, 27, 28]. Cooling allows the system to reach supersaturation, maintaining the same concentration - this is clear in figure 2. Although it

is only efficient to use when the solubility of the compound greatly decreases with temperature [29, 30]. Adding anti-solvent reduces the solubility of the compound, making it easier to reach supersaturation. Furthermore, anti-solvent addition has been claimed as the most efficient strategy to reach supersaturation as it is quicker and able to run at low temperatures [31, 30]. Solvent evaporation is used when the solubility curve is quite flat, making it unfeasible to achieve supersaturation by cooling [29], despite being a less common alternative [32]. Lastly, another method to induce supersaturation is by pH change, an option used in protein crystallization [33].

3. Materials and Methods

The modelling tool used was the gPROMS FormulatedProducts, a platform which integrates formulated products with their manufacturing process, from pharmaceutical products, to agrochemicals and food products. It includes several libraries; the one used for the current project is named gCRYSTAL. This library provided the model to which the control strategy was used. The control strategy was implemented on gNLMPC, a gPROMS digital application platform, that allows the controller's configuration, tuning and deployment.

4. Model Description

The model used depicts a batch crystallization of paracetamol, where the crystal seeds are added at the beginning of the batch. The main mechanisms included in the simulation are secondary nucleation, growth and dissolution and agglomeration. Only secondary nucleation by attrition was considered (as the primary one does not occur in industry), following a custom kinetics scheme, of empirical nature given by [34]:

$$J_{sec} = k_n \, (C - C_*)^n \, \mu_2^{n_{sec}} \tag{1}$$

Where J_{sec} is the rate of nucleation, C is the solute concentration. C_* the solubility, k the nucleation rate constant, n the nucleation order and n_{sec} the second nucleation order.

Likewise, growth, dissolution also follow a custom kinetics scheme [34]:

$$G = k_g \, (C - C_*)^g \tag{2}$$

Where G is the growth and dissolution rate, k is the growth rate constant and g the growth order.

Agglomeration is described by an empirical power law of the form [34]:

$$\beta_{agg} = a_1 G^{a_2} \varepsilon^{a_3} \tag{3}$$

Where β_{agg} is the agglomeration rate, a_1, a_2 and a_3 are empirical parameters and ε is defined by:

$$\varepsilon = \frac{N_p \, d_{imp}^5 \, n_s^3}{V} \tag{4}$$

In which N_p is the stirrer's power number, d_{imp} the impeller diameter, n_s the stirring rate and V the reactor volume.

Anti-Solvent Flow and temperature were chosen as MVs as they are the main drivers for supersaturation, and, consequently, crystallization. Typical goals for crystals include achieving maximum growth with minimum particle size dispersion. Hence, variables such as span and volume mean size were the chosen metrics of that goal. Span is a measure of particle size dispersion and volume mean size is defined as the mean volume of particles divided by their diameter, which can be a measure of the crystals' growth. Relative supersaturation was chosen to be a CV in order to ensure the correct crystallization conditions are being met. Lastly, dissolved paracetamol was chosen as a CV to keep track of the crystallization progress and to guarantee that there is paracetamol left to react. Impeller frequency was chosen as the sole DV as it is a independent variable to the system, meeting the general criteria for this kind of variable.

5. Optimisation

The control objectives were expressed as the desired interval of values for the CVs, at the end of the batch, since constructing a controller to comply with specific values may be deemed too conservative, while also making the optimisation procedure rather burdensome, as the optimal solution would take longer to be found. The objective function that describes the optimisation problem is penalty-based, which means that penalties are added whenever a CV is outside its desired interval. The interval of values chosen are the ones intended for the CV at the end of the batch operation. In this way, the controller ensures that these variables comply with control objectives for that batch. The penalties added for the violation of these limits are different for each CV: this ensures the controller prioritizes some objectives over others.

Additional terms may be added to the objective function to penalize a CV heading to its desired limits too fast or to penalize a MVs that is either changing too much within or between cycles.

The objective function used in the present work

is defined by equation 5 [35].

$$\min_{u_{i,k}|\lambda_i^u=1} OF \equiv \sum_{j\in CV} \lambda_j^z \, {C'}_j^{z,lo} \int_0^{T^{opt}} \max(0, z_j^{ref,lo}(t) - \bar{z}_j(t))^2 \, dt + \sum_{j\in CV} \lambda_j^z \, {C'}_j^{z,hi} \int_0^{T^{opt}} \max(0, z_j^{ref,hi}(t) - \bar{z}_j(t))^2 \, dt + \sum_{j\in CV} \lambda_j^z \, C_j^z \int_0^{T^{opt}} \bar{z}_j(t) \, dt + \sum_{i\in MV} \lambda_i^u \, C_i^u \sum_{k=1} \delta_k \, u_{i,k} + \sum_{i\in MV} \lambda_i^u C_i^{\delta u} \sum_{k=1}^{K} |u_{i,k} - u_{i,k-1}| \quad (5)$$

where OF is the objective function, CV the controlled variable, MV the manipulated variable, T^{opt} the optimization time horizon, K the number of control intervals, δ_k the duration of control intervals, $u_{i,k}$ the MV value i over control interval k, λ_i^u the binary switch (0/1) indicating whether MV i is included in the optimisation, λ_j^z the binary switch (0/1) indicating whether CV i is included in the optimisation, ${C'}_j^{z,lo}$ and ${C'}_j^{z,hi}$ the violation penalties applied to CV when it is below or above its reference envelope limits, $z_j^{ref,lo}(t), z_j^{ref,hi}(t)$ the lower and upper limits of reference envelopes, $\bar{z}_j(t)$ the CV trajectory, C_j^z the CV j cost penalty, C_i^u the MV i cost penalty and $C_i^{\delta u}$, the MV i cost penalty at control interval boundaries. In the above formulation, the optimisation time horizon T^{opt} is defined by the sum of the control intervals K, of length δ_k.

6. Results

The controller was tested in emulation mode, which is the real-time implementation of the controller's optimal control action on a digital twin of the model. The tuning of the controller consisted in changing one the of model's parameters and studying its impact on both CVs and MVs. The testing included submitting the controller to several scenarios. One of them was performing $\pm$ 5% step changes on the disturbance variable, impeller frequency, on the second cycle of a 20-cycle emulation.

6.1. Disturbance Rejection

The measured and optimal trajectories for one of the CVs, dissolved paracetamol are presented below in figure 3. The dotted blue line represents the closed-loop control trajectories (with the controller active), the orange one the open-loop trajectories (with the controller inactive) and the grey line the optimal trajectory (predicted by the controller). The dashed lines represent the lower and upper bounds of the reference envelopes.

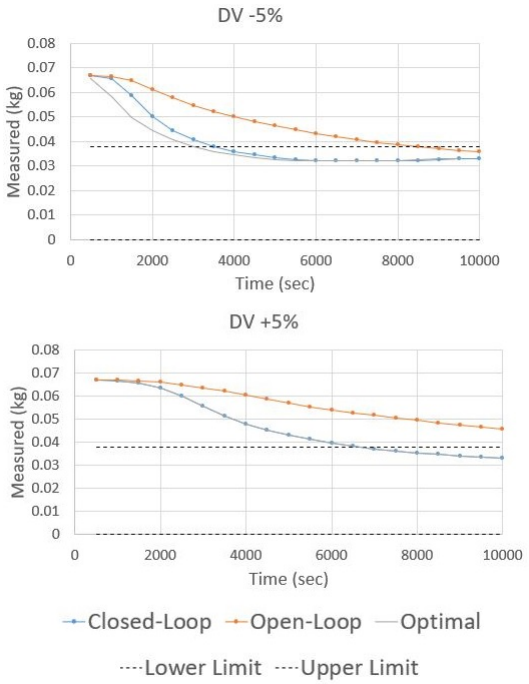

Figure 3: Paracetamol Liquid Mass measured and optimal trajectories for the different disturbance rejection tests

The presented variable is able to be steered into its reference envelopes for all disturbances, thus, confirming the controller's ability to meet the control objectives. An interesting aspect to note is that not only is the closed-loop trajectory faster than the open-loop one, but also for the +5% case, the open-loop trajectory does not even reach its reference envelope, at the end of the batch. This means that for this case in particular, the control objectives would not be met, if it were not for the controller. This case clearly shows the benefit of having implemented such control strategy, as reaching the reference envelopes faster translates into a faster crystallization, because it means that paracetamol is transforming into crystals sooner. Furthermore, in the -5% case, there is a mismatch between the optimal and closed-loop trajectories. However, for the other case, there is perfect match between the two. This confirms the controller's ability to predict this CV response to the control action implemented. The slight observed mismatch is only visible in the first cycles. This shows that the controller may predict that its actions have an instantaneous impact of the model, thus not taking into account some delay.

In figure 4, the MVs trajectories are displayed. Anti-Solvent Flow heads to its upper limit and settles there for the entire emulation. One

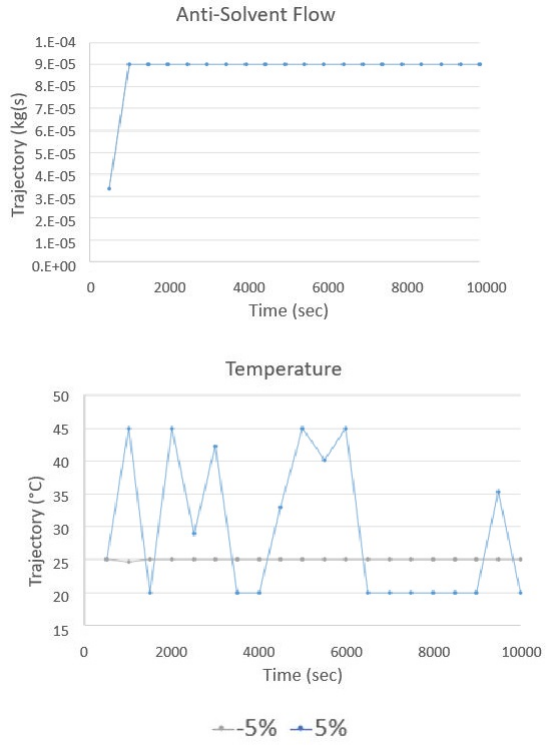

Figure 4: Manipulated Variables measured trajectories for the different disturbance rejection tests

hypothesis for this behaviour is that settling in its upper limit is the optimal solution that maximizes crystal growth. As long as other control objectives, such as particle disparity, are achieved, the controller can promote crystal growth by increasing anti-solvent flow.

Yet the same is not observed for temperature. A + 5 % disturbance barely changes this MV out of its initial value of 25 °C. For the - 5 % case, temperature oscillates between its bounds (from 20 to 45 °), sometimes from one cycle to another.

Both MVs' optimal trajectories would not be feasible in reality as the anti-solvent flow could not increase so abruptly in one single cycle, and temperature could not swing as much either. In both cases, the actuators would not be able to implement these changes so quickly, which would mean that the system would not receive them either. This would result in increasing the plant / model mismatch, as the controller would not take into account this delay. In case of the temperature, this problem would be even more serious as the changes are not from one cycle to another, this oscillation happens throughout the emulation. So the sensors would measure a temperature, which would not be true by the time this measurement reached the controller. This would lead to the controller receiving past information, when performing its optimisation routine. In order to tackle this issue, a rate of change penalty was added to the MVs. The results for both this option will be shown below.

6.2. Rate of Change Penalty

The term C in the objective function (equation 5) was activated - this meant choosing the parameters $C_i^{\delta u}$ and $|u_{i,k} - u_{i,k-1}|$, which are the penalties applied to the rate of change and the maximum rate of change allowed per cycle. Adding a penalty to the rate of change is the way to tell the controller to find a new solution that avoids a rapid change between variables. The rate of change per cycle refers to the maximum change the controller allows for that variables, between cycles.The rates and penalties applied in each MV are shown in table 1.

Table 1: Rate of change and penalties for both MVs

Variable	Rate of change per cycle	Penalty
Anti-Solvent Flow	1E-5 kg/s	1E5
Temperature	1 °C	1

The rate of change penalty for temperature was chosen according to literature [27]. The penalty difference between variables is not due to importance but for scaling reasons, given that the objective function is not scaled.

A -5% disturbance step was performed and the differences between the original case without rate of change penalties and the modified one with the penalty were compared. The MVs trajectories are shown below:

It is possible to verify that the addition of a penalty was successful, as anti-solvent flow takes more time to reach its optimal value and temperature shows a lower degree of oscillation. It is also worth noting that whereas temperature effectively oscillates less, meaning another optimal solution was found, different from the original one, regarding anti-solvent flow, this does not hold true. Given that this variable changes its maximum allowed per cycle, one can conclude that the controller was not able to find a new optimal solution, but instead just complied with the penalties given.

The next aspect to verify was whether the controller had been able to achieve the desired control targets despite the penalties. The CVs trajectories are depicted in figure 6.

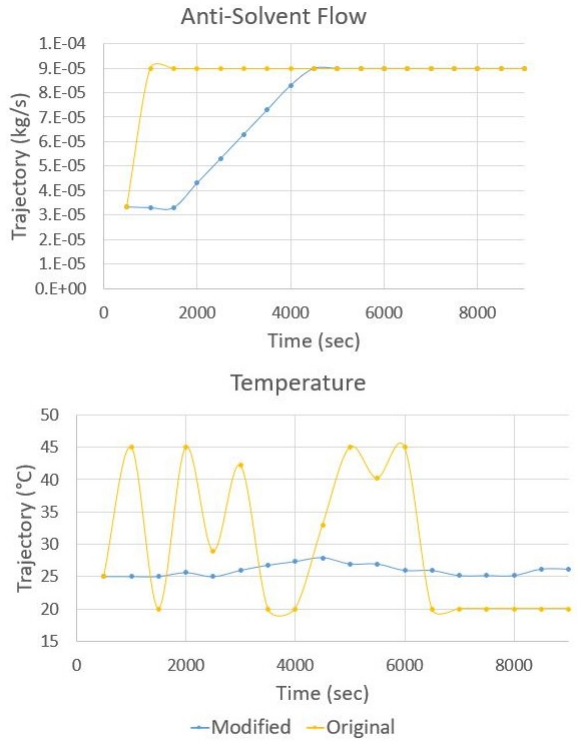

Figure 5: Manipulated Variables measured trajectories with and without the rate of change penalty

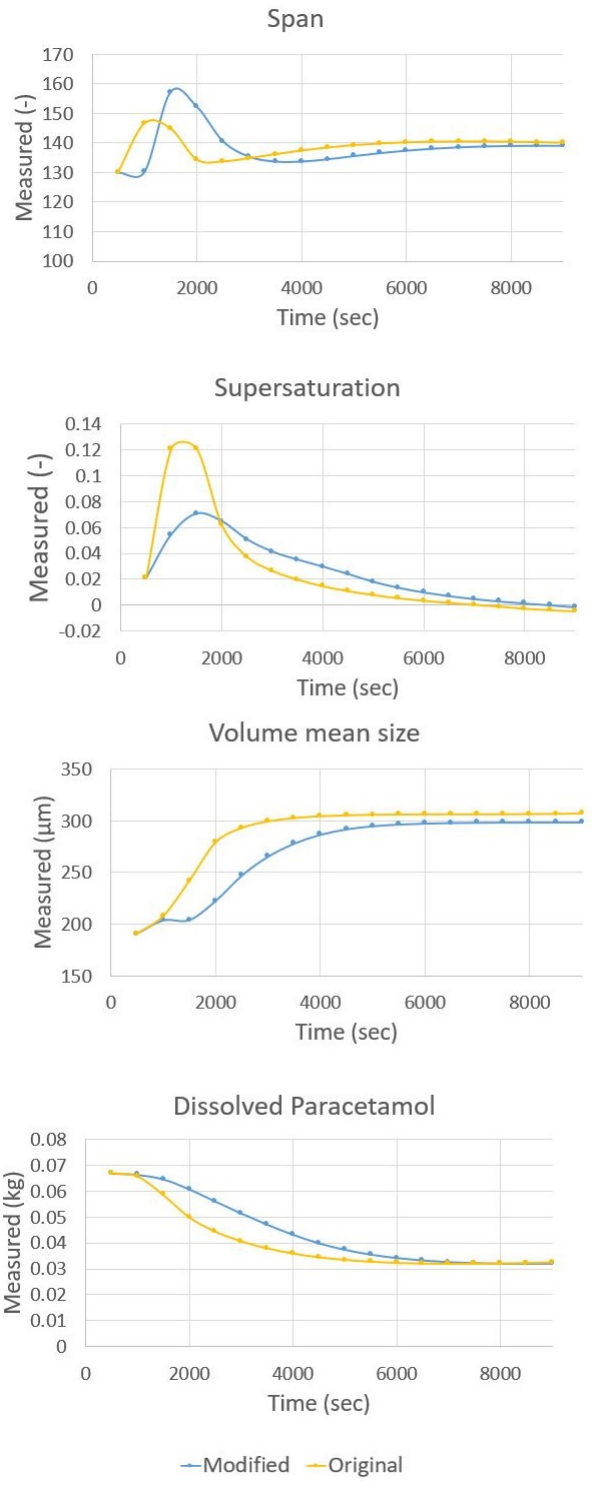

Figure 6: CVs trajectories with and without the rate of change penalty

As expected, the CVs were affected by the change: in the modified case, the trajectories show a slight delay when compared to the original case. Nonetheless, with the exception of volume mean size, in both cases, the end-point is similar, which seems to indicate that the delay the penalties added did not prevent the controller from reaching its goals. The fact that the rate of change penalty made the variables rate of change slower confirms the optimality of the original solution, as it lead the CVs sooner to their reference envelopes, which is an advantage.

As it has been observed previously, anti-solvent flow seems to be tendentiously hitting its upper bound, in many of the scenarios tested. Thus, a global system analysis was conducted in order to find an explanation as to why the anti-solvent flow always hit its upper bound. This gPROMS feature is essentially a sensitivity analysis where the relationships between some input variables (called factors) and output variables (called responses) are analysed. The input variables are changed within some specified bounds and the impact on the responses is analysed. For this global system analysis, anti-solvent flow was chosen as a factor and the CVs as responses. The results are shown in figure 7.

One can see that maximum anti-solvent flows clearly maximizes volume mean size and minimizes supersaturation, which were the control objectives for these CVs. These were possibly the main factors contributing to this MV hitting its upper bound. Another CV, span, shows an oscillating relation with anti-solvent flow, inside a narrow range of values. Hence, it may not have contributed so bluntly as the previous two CVs.

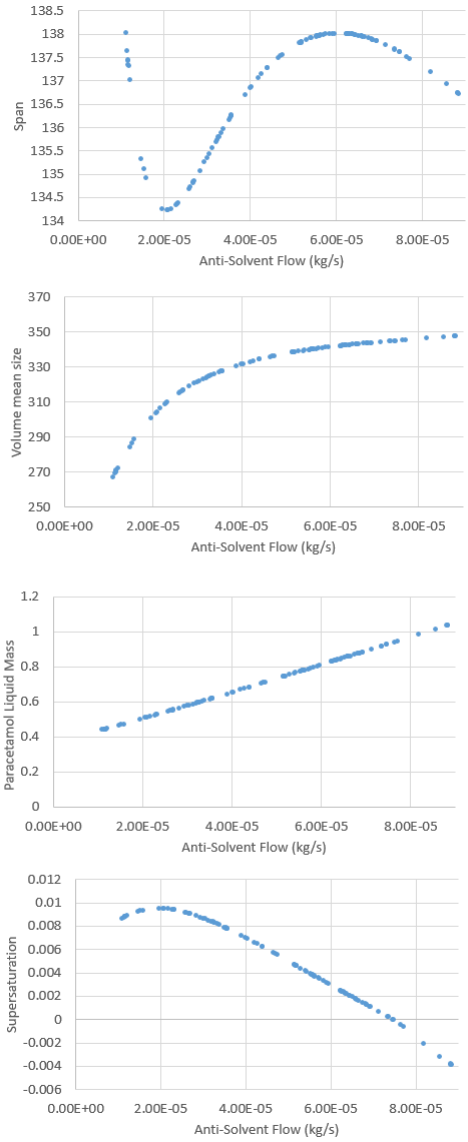

Figure 7: Global System Analysis Results - Responses

Due to the non linear nature of the relationship between these two variables, the controller had more difficulty in choosing the correct anti-solvent flow that satisfied the span's control objectives.

Furthermore, lower anti-solvent flow values led to less dissolved paracetamol at the end of the batch. Nonetheless, given this was a secondary objective (reaching Particle Size Distribution goals like volume mean size was more important), a minor penalty was implemented, thus, the controller values did not show this tendency.

The sensitivity analysis confirmed that the controller was implementing the values more suitable for the anti-solvent flow, given that they are in agreement with the control objectives.

6.3. Noise Measurement

The controller's ability to handle noise was tested next. Noise was added to one of the measurements, which is also a CV, span. Step changes on DV impeller frequency were performed (similarly to the ones done in section 6.1), and compared the original case with the case with the noise added. The CV trajectories for both cases is shown below (figure 8).

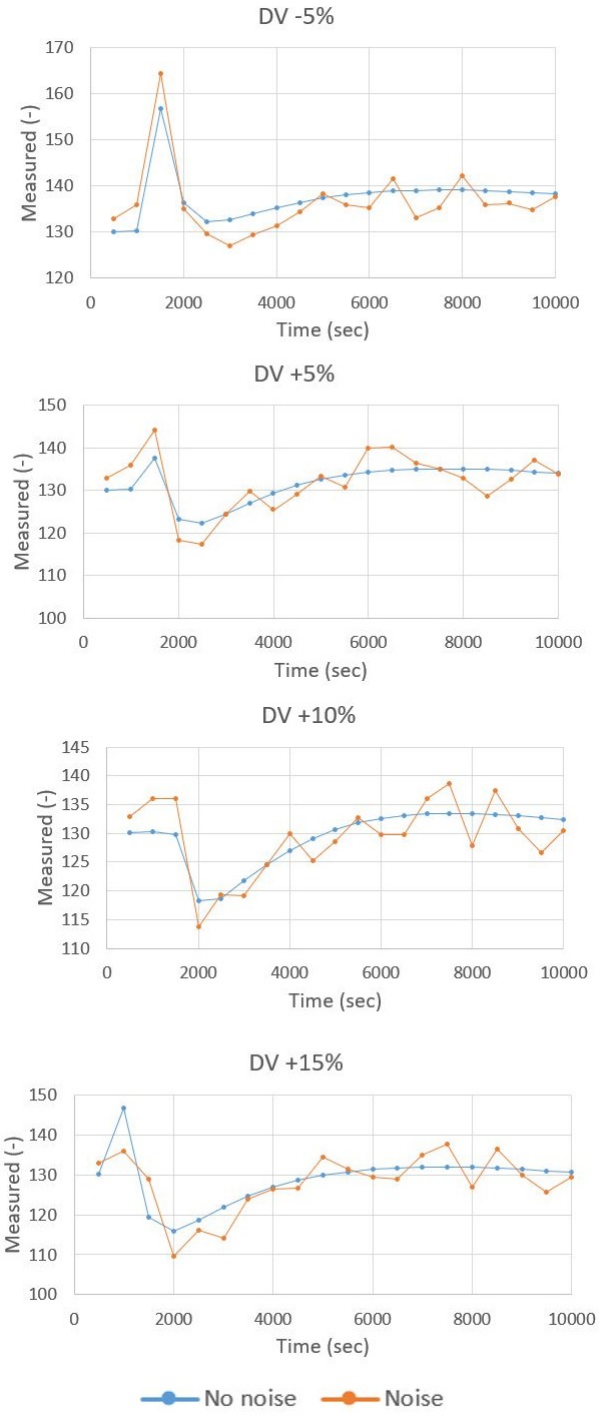

Figure 8: CV span with and without noise

From figure 8, it is possible to verify that the

noise was successfully added to the CV, as its trajectory shows a higher degree of fluctuation, when compared to its original trajectory. In spite of having noise, this CV still ended the batch in the same point as the original case. This indicates that the controller was able to accomplish the targets and perform noise rejection.

The trajectory of the MV anti-solvent flow is not shown as the addition of noise did not affect this variable's values (in all cases, this variable hit its upper bounds, as expected). However, temperature showed different trajectories, depicted by figure 9.

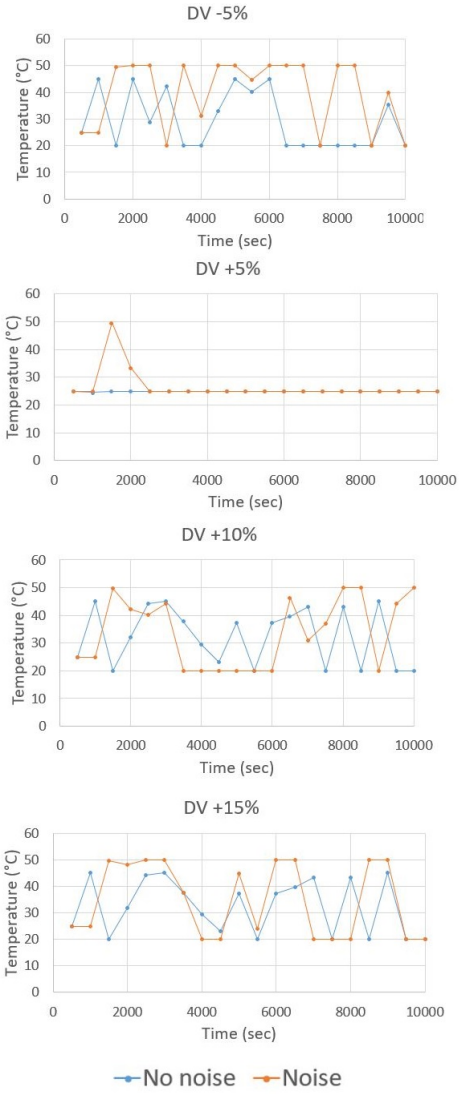

Figure 9: MV temperature with and without noise

In both cases (with and without added noise), temperature shows quite some oscillation.. For a $\pm$ 5% disturbance change, the case with added noise seems to have more oscillation. For the + 10 and 15% both scenarios, with and without noise, display the same degree of oscillation, without a clear pattern.

A controller able to tackle measurement noise rejection is a clear advantage. In the current case, this variable was not only a CV, but the most nonlinear one, as it was possible to verify in the sensitivity analysis shown before. This points to the overall good performance of the controller in handling noise measurement rejection.

7. Conclusions

The main goal of implementing a Nonlinear Model Predictive Control application on a batch crystallization of paracetamol model was successfully achieved.

The controller was tested on a digital twin of the model, which is the real-time implementation of the controller on the process. The testing consisted in submitting the controller to different scenarios to verify whether it was able to steer the Controlled Variables into their target limits, thus, achieving their control objectives. Tested scenarios included disturbance rejection (changing Disturbance Variable impeller frequency) and noise measurement (adding noise to one of the measured variables, Span) . The controller was able to successfully steer the Controlled Variables for most cases, yielding faster results than in open-loop mode. Reaching control objectives faster than in open-loops proves to be an advantage as it can translate in ending a batch sooner, thus saving time.

In one of the disturbance rejection tests, the controller's optimal trajectories for the manipulated variables were not feasible in a real plant, as they changed too fast from one cycle to another. Hence, a rate of change penalty between cycles was added. Having done this, the controller was able to, not only keep achieving its control objectives, but it was also able to comply with the penalties submitted, smoothing the optimal trajectories for the MVs.

A sensitivity analysis showed the importance of choosing the correct limits of operability for the Manipulated Variables, as Anti-Solvent Flows showed the tendency of clipping to its upper bound for most scenarios tested, as it maximized crystal growth (one of the control objectives).

Overall, the controller yielded quite satisfactory results, showing a promising future for this less commonly used control strategy.

References

[1] M. Skliar, "Process dynamics and control, 2nd edition by dale e. seborg, thomas f. edgar, and duncan a. mellichamp," *AIChE Journal*, vol. 54, 11 2008.

[2] J. Rossiter, *Model-based Predictive Control-a Practical Approach*. CRC Press, 01 2003.

[3] R. Findeisen, L. Imsland, F. Allgower, and B. A. Foss, "State and output feedback nonlinear model predictive control: An overview," *European Journal of Control*, vol. 9, no. 2, pp. 190 – 206, 2003.

[4] O. Mikuláš, "A framework for nonlinear model predictive control," Master's thesis, The school of the thesis, The address of the publisher, 7 1993. An optional note.

[5] F. Allgöwer, T. Badgwell, J. Qin, J. B. Rawlings, and S. J. Wright, *Nonlinear Predictive Control and Moving Horizon Estimation – An Introductory Overview*, pp. 391–449. 01 1999.

[6] J. Bausa, "Model based operation of polymer processes – what has to be done?," *Macromolecular Symposia*, vol. 259, no. 1, pp. 42–52, 2007.

[7] P. Kühl, M. Diehl, A. Milewska, E. Molga, and H. Bock, *Robust NMPC for a Benchmark Fed-Batch Reactor with Runaway Conditions*, vol. 358, pp. 455–464. Springer, 08 2007.

[8] K. Naidoo, J. Guiver, P. Turner, M. Keenan, and M. Harmse, *Experiences with Nonlinear MPC in Polymer Manufacturing*, pp. 383–398. Berlin, Heidelberg: Springer Berlin Heidelberg, 2007.

[9] R. Bindlish, "Nonlinear model predictive control of an industrial polymerization process," *Computers & Chemical Engineering*, vol. 73, pp. 43–48, 2015.

[10] S. Skålén, F. Josefsson, and J. Ihrström, "Nonlinear mpc for grade transitions in an industrial ldpe tubular reactor," *IFAC-PapersOnLine*, vol. 49, pp. 562–567, 12 2016.

[11] B. Foss and T. Schei, *Putting Nonlinear Model Predictive Control into Use*, vol. 358, pp. 407–417. 08 2007.

[12] R. D. Bartusiak and R. W. Fontaine, "Feedback method for controlling non-linear processes," Oct 1997.

[13] M. W. Hermanto, M.-S. Chiu, and R. D. Braatz, "Nonlinear model predictive control for the polymorphic transformation of l-glutamic acid crystals," *AIChE Journal*, vol. 55, no. 10, pp. 2631–2645, 2009.

[14] C. Damour, M. Benne, L. Boillereaux, B. Grondin-Perez, and J.-P. Chabriat, "Nmpc of an industrial crystallization process using model-based observers," *Journal of Industrial and Engineering Chemistry - J IND ENG CHEM*, vol. 16, pp. 708–716, 09 2010.

[15] L. A. P. Suárez, P. Georgieva, and S. F. de Azevedo, "Nonlinear mpc for fed-batch multiple stages sugar crystallization," *Chemical Engineering Research and Design*, vol. 89, no. 6, pp. 753 – 767, 2011.

[16] D. Sarabia, C. Prada, S. P. Cristea, R. Mazaeda, and W. Colmenares, *Hybrid NMPC control of a sugar house*, vol. 358, pp. 495–502. 09 2007.

[17] Y. Cao, J. Kang, Z. K. Nagy, and C. D. Laird, "Parallel solution of robust nonlinear model predictive control problems in batch crystallization," *Processes*, vol. 4, p. 20, 06 2016.

[18] R. D. Braatz, "Advanced control of crystallization processes," *Annual Reviews in Control*, vol. 26, no. 1, pp. 87 – 99, 2002.

[19] A. Mesbah, Z. K. Nagy, A. E. M. Huesman, H. J. M. Kramer, and P. M. J. Van den Hof, "Nonlinear model-based control of a semi-industrial batch crystallizer using a population balance modeling framework," *IEEE Transactions on Control Systems Technology*, vol. 20, pp. 1188–1201, Sep. 2012.

[20] N. C. S. Kee, R. B. H. Tan, and R. D. Braatz, "Selective crystallization of the metastable α-form of l-glutamic acid using concentration feedback control," *Crystal Growth & Design*, vol. 9, no. 7, pp. 3044–3051, 2009.

[21] M. Giulietti, M. Seckler, S. Derenzo, M. RÃ©, and E. Cekinski, "INDUSTRIAL CRYSTALLIZATION AND PRECIPITATION FROM SOLUTIONS: STATE OF THE TECHNIQUE," *Brazilian Journal of Chemical Engineering*, vol. 18, pp. 423 – 440, 12 2001.

[22] N. A. Mitchell, "Numerical modelling of cooling crystallisation: process kinetics to optimisation," 2012.

[23] M. W. Hermanto, "Modelling, simulation, and control of polymorphic crystallization," 2009.

[24] A. D. RANDOLPH and M. A. LARSON, "Chapter 6 - crystallization kinetics," in *Theory of Particulate Processes* (A. D. RANDOLPH and M. A. LARSON, eds.), pp. 101 – 110, Academic Press, 1971.

[25] W. Beckmann, *Crystallization: Basic Concepts and Industrial Applications*, pp. 173–185. 02 2013.

[26] Z. K. Nagy and R. D. Braatz, "Advances and new directions in crystallization control," *Annual Review of Chemical and Biomolecular Engineering*, vol. 3, no. 1, pp. 55–75, 2012. PMID: 22468599.

[27] Y. Yang and Z. K. Nagy, "Advanced control approaches for combined cooling/antisolvent crystallization in continuous mixed suspension mixed product removal cascade crystallizers," *Chemical Engineering Science*, vol. 127, p. 362–373, 05 2015.

[28] M. Kitamura, "Strategy for control of crystallization of polymorphs," *Crystengcomm*, vol. 11, 05 2009.

[29] Baliga and J. Bantwal, "Crystal nucleation and growth kinetics in batch evaporative crystallization," 06 2019.

[30] C. Lindenberg, M. Krattli, J. Cornel, and M. Mazzotti, "Design and optimization of a combined cooling/antisolvent crystallization process," *Crystal Growth & Design - CRYST GROWTH DES*, vol. 9, 12 2008.

[31] C. T. Ó'Ciardhá, N. A. Mitchell, K. W. Hutton, and P. J. Frawley, "Determination of the crystal growth rate of paracetamol as a function of solvent composition," *Industrial & Engineering Chemistry Research*, vol. 51, no. 12, pp. 4731–4740, 2012.

[32] K. Choong and R. Smith, "Novel strategies for optimization of batch, semi-batch and heating/cooling evaporative crystallization," *Chemical Engineering Science*, vol. 59, no. 2, pp. 329 – 343, 2004.

[33] C. Ruiqing, Q.-d. Cheng, J. J. Chen, D.-S. Sun, L.-b. Ao, D.-W. Li, Q.-Q. Lu, and D.-C. Yin, "An investigation of the effects of varying ph on protein crystallization screening," *CrystEngComm*, vol. 19, 01 2017.

[34] C. T. Ó'Ciardhá, K. W. Hutton, N. A. Mitchell, and P. J. Frawley, "Simultaneous parameter estimation and optimization of a seeded antisolvent crystallization," *Crystal Growth & Design*, vol. 12, no. 11, pp. 5247–5261, 2012.

[35] R. E. Young, R. Donald Bartusiak, and R. W. Fontaine, "Evolution of an industrial nonlinear model predictive controller," *Proc. of Chem Process Control VI*, vol. 6, 01 2002.